ACCOUNTS
of chemical research

Custom-Designed Nanomaterial Libraries for Testing Metal Oxide Toxicity

SUMAN POKHREL,[†] ANDRÉ E. NEL,[‡] AND LUTZ MÄDLER*,[†]

[†]*Foundation Institute of Materials Science (IWT), Department of Production Engineering, University of Bremen, Germany, and* [‡]*Department of Medicine-Division and California NanoSystems Institute, University of California, Los Angeles, California, United States*

RECEIVED ON JANUARY 29, 2012

CONSPECTUS

Advances in aerosol technology over the past 10 years have enabled the generation and design of ultrafine nanoscale materials for many applications. A key new method is flame spray pyrolysis (FSP), which produces particles by pyrolyzing a precursor solution in the gas phase. FSP is a highly versatile technique for fast, single-step, scalable synthesis of nanoscale materials. New innovations in particle synthesis using FSP technology, including variations in precursor chemistry, have enabled flexible, dry synthesis of loosely agglomerated, highly crystalline ultrafine powders (porosity $\geq$ 90%) of binary, ternary, and mixed-binary-and-ternary oxides. FSP can fulfill much of the increasing demand, especially in biological applications, for particles with specific material composition, high purity, and high crystallinity.

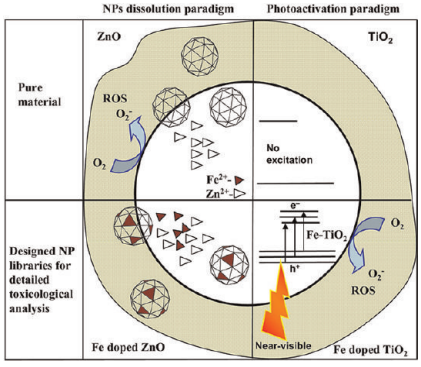

In this Account, we describe a strategy for creating nanopartide libraries (pure or Fedoped ZnO or TiO_2) utilizing FSP and using these libraries to test hypotheses related to the particles' toxicity. Our innovation lies in the overall integration of the knowledge we have developed in the last 5 years in (1) synthesizing nanomaterials to address specific hypotheses, (2) demonstrating the electronic properties that cause the material toxicity, (3) understanding the reaction mechanisms causing the toxicity, and (4) extracting from in vitro testing and in vivo testing in terrestrial and marine organisms the essential properties of safe nanomaterials.

On the basis of this acquired knowledge, we further describe how the dissolved metal ion from these materials (Zn^{2+} in this Account) can effectively bind with different cell constituents, causing toxicity. We use Fe–S protein clusters as an example of the complex chemical reactions taking place after free metal ions migrate into the cells.

As a second example, TiO_2 is an active material in the UV range that exhibits photocatalytic behavior. The induction of electron–hole (e^-/h^+) pairs followed by free radical production is a key mechanism for biological injury. We show that decreasing the bandgap energy increases the phototoxicity in the presence of near-visible light. We present in detail the mechanism of electron transfer in biotic and abiotic systems during light exposure. Through this example we show that FSP is a versatile technique for efficiently designing a homologous library, meaning a library based on a parent oxide doped with different amounts of dopant, and investigating the properties of the resulting compounds.

Finally, we describe the future outlook and state-of-the-art of an innovative two-flame system. A double-flame reactor enables independent control over each flame, the nozzle distances and the flame angles for efficient mixing of the particle streams. In addition, it allows for different flame compositions, flame sizes, and multicomponent mixing (a grain–grain heterojunction) during the reaction process.

Introduction

Many industrial sectors such as catalyst manufacturing, composite materials or passive electronic components include nanoparticles (NPs) in their processes. The market for nanotechnology based electronic components and pharmaceuticals was $147 billion in 2007 and is expected to reach $2.5 trillion by 2015.[1,2] Over the past decade, newly developed NPs have been found to exhibit fascinating properties.[3] The development in NP production, especially their specific design, was mostly realized during the last 20 years. Initially, wet chemical

Published on the Web 11/29/2012 www.pubs.acs.org/accounts
10.1021/ar300032q

routes were used for the preparation of oxide materials.[4,5] Adapted from manufacturing of carbon black, the almost 70 years old industrial aerosol flame process was always a part of alternative methods for NP production. This dry synthetic method has advantages such as high purity and continuous production at high rates but was limited for a long time to simple metal oxides such as TiO_2, Al_2O_3, and SiO_2. Flame spray pyrolysis (FSP) was developed in the past decade and has developed into a very versatile technique in this family.[6] The spectrum of NPs that can be produced is greatly enhanced with the FSP process that relies on the direct introduction of a liquid precursor into the flame, producing highly dispersed, ultrafine, and single crystalline NPs.[7] Due to the enormously broad range of precursors available, FSP is one of the most promising single-step techniques for the synthesis of a large class of binary, mixed binary, ternary, and mixed ternary metal oxide NPs.[6] This method overcomes the difficulty of bulk production and the complex chemical reactions involved. For example, synthesizing mixed oxide catalysts using precipitation method often involves the change of pH. However, the required pH can be very different for different oxide materials (e.g., Al_2O_3 and MgO), leading to a process with multiple precipitation steps. With the FSP method, however, complex mixtures are possible in a single step. Furthermore, this approach enables efficient in situ manufacturing of NP layers and their patterning on different substrates.[8] The state-of-the-art for designing homologous NP libraries (parent oxide doped with different amount of dopant) using versatile FSP technique is described in the Supporting Information.

Due to the small size of the NPs compared to their bulk counterparts, they have a large number of surface atoms and therefore offer increased reactivity that enhances electron transfer, efficiently binds molecular species, and easily translocates cell membranes when they are exposed to humans and the environment.[9] In accordance to their attractive properties, NPs are utilized in advanced applications such as drug and gene delivery, biosensing, virus inhibition, and protein immobilization.[10] These extraordinary properties, however, can in most cases not be deactivated at will. They are therefore omnipresent until the properties change due to environmental factors that can, for example, lead to agglomeration. The increased use of nanoscale materials might lead to increased likelihood of environmental and human exposure and has already raised concerns about their short- and long-term toxicological and ecological effects.[11] Therefore, screening NPs toxicity for environmental implication becomes an important tool to predict possible biological injuries.[12] High content screening (search for chemical entities modulating important processes that can be imaged in biologically relevant cellular systems) permits parallel measurements of multiple parameters characterizing the cellular phenotype.[13] Such considerations are being set in place before the commercial production of new nanoscale materials, exposure potential at work places, handling by the consumer, and their final disposal.[14]

Custom Designing ZnO or TiO_2 NP Libraries Using FSP

The current research activities on flame aerosol synthesis aim at developing cost-efficient routes to new and functional multicomponent and metastable NPs with the increased understanding of the chemical and physical principles underlying this process. In the flame environment, reactions and particle growth take place within milliseconds at high temperatures and the ability to rapidly quench these NPs provides possibilities for doping metal oxides beyond their solubility limit and for creating metastable high temperature phases.[8] FSP is an attractive method (Figure S1, Supporting Information) for NP production as it enables the use of wide range of precursors for different metal oxides. Particles can be re-engineered efficiently because each precursor droplet contains the same content of metals as desired in the product. In flame aerosol reactors, the energy of the flame generates the conditions for the NP growth, crystallization, and morphological structure. The particles are formed in the gas phase through nucleation, surface growth, coagulation, and coalescence[15,16] in the flame environment during combustion of the dispersed droplets. The nanoparticle aerosol is collected after the particles are quenched to room temperature.[17]

In this Account, we focus on the designing combinatorial NP library (pure or Fe doped ZnO/TiO_2) and their high content screening process.[12] The choice of these materials to develop and evaluate the screening process was based on the demonstration of their differential toxic effects in a series of cellular assays.[18] The cytotoxic and proinflammatory effects of ZnO particles are related to particle dissolution intra- and extracellularly.[18] Particle generated ROS leads to a range of biological responses depending on the relative abundance of ROS and the type of cellular pathways that are induced through oxidative stress.[11]According to the hierarchical oxidative stress (OS), the lower OS includes activation of the antioxidant response element in the promoters of phase II genes by the transcription factors (Figure 1e–g) leading to the expression of cytoprotective enzymes.[18] Only ZnO could generate a robust HO-1 message

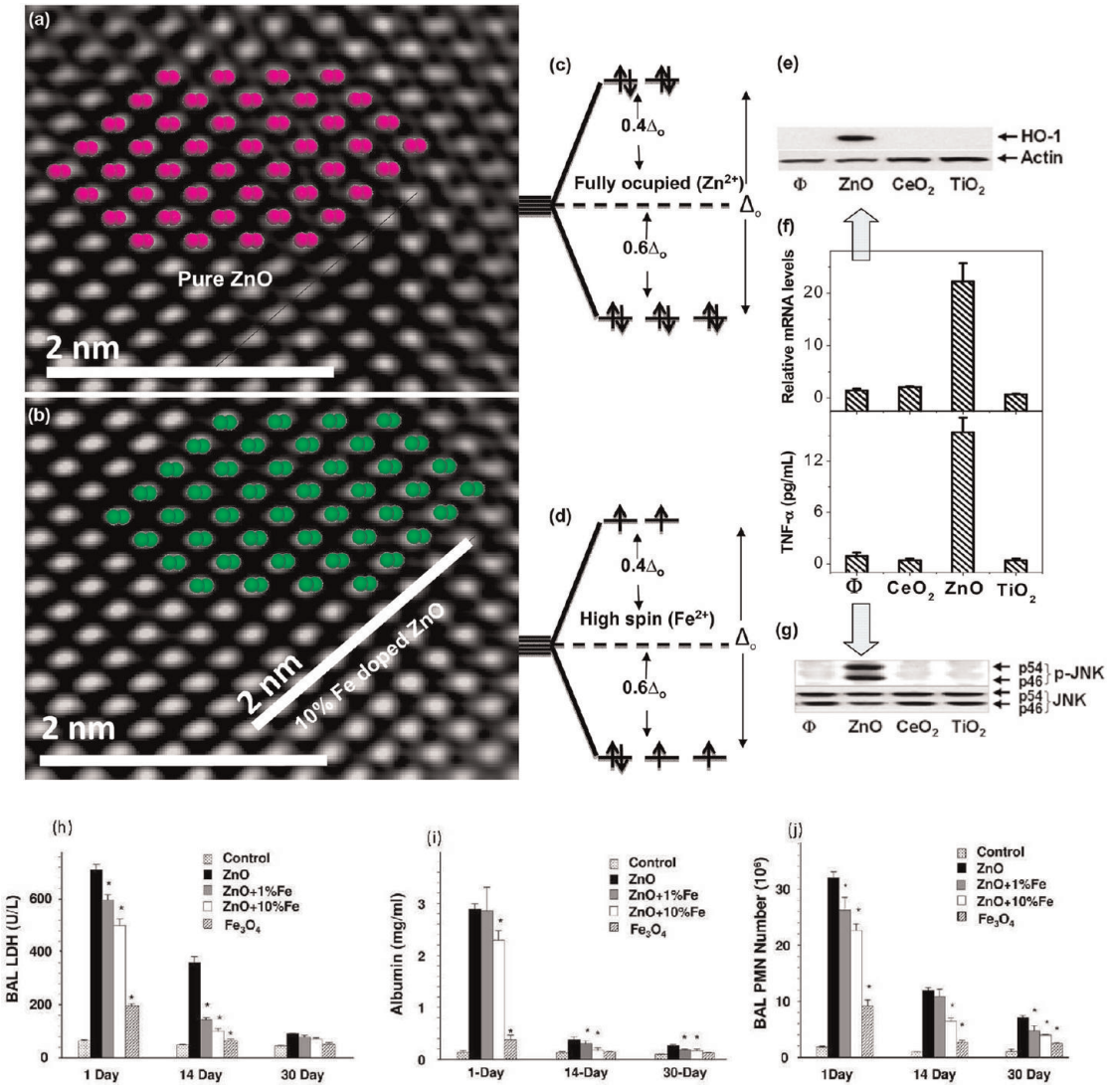

FIGURE 1. Physicochemical characterization of undoped and Fe doped ZnO NPs. (a,b) Matching crystal structure with HRTEM image for undoped and Fe doped ZnO. No detectable structural deviation observed (c,d). d-Orbitals splitting of Zn^{2+} and Fe^{2+} (e−g). Induction of OH-1 expression and Jun kinase activation by immuno-blotting and TNF-activation of ZnO, CeO_2, or TiO_2 (h−j). Time dependent toxicity evaluation. Animals were euthanized, and BAL fluid was collected to determine PMN numbers, LDH, and albumin levels (Supporting Information). (Reprinted in part with permission from refs 18 and 19. Copyright 2008 and 2011 American Chemical Society.)

and protein expression in RAW 264.7 cells. The time dependent in vivo results show that (LDH) release, PMN cell count, and albumin level decreased with Fe content (Figure 1h−j).

We hypothesized that a change in NP dissolution characteristics through iron doping should lead to decreased toxicity that could be assessed through HCS. Microscopic results [high resolution TEM, electron diffraction (SAED)] and X-ray diffraction (XRD) confirmed that 10% iron loadings are possible without any detectable differences in the lattice spacing. To experimentally verify this, HRTEM image of pure ZnO with hexagonal arrangement of the lattices was structurally matched (Figure 1a,b) with the crystal structure of ZnO and Fe doped ZnO. The perpendicular rows with respective *d*-spacing of 2.47(±0.008) Å reasonably agree with d_{011} = 2.476 Å from XRD for both ZnO and Fe doped ZnO. A structure plot created for ZnO and Fe doped ZnO in a projection along (011) direction superimposed to high-resolution image of ZnO shows that the heavy atoms (oxygen atoms are omitted for clarity) of both structures reasonably match suggesting no detectable variations. Results from energy filtered TEM (EFTEM) show Fe is homogeneously distributed in the ZnO lattice. The dissolution of ZnO or Fe doped ZnO in aqueous solution performed in electrolyte solution was studied by adding 0.1 M $NaClO_4$ at pH 7 (±0.04) and 22 °C. The reaction [$ZnO_{(s)} + 2H^+ \rightarrow Zn^{2+}{}_{(aq)} + H_2O_{(l)}$] was followed by periodic sampling of aliquots for total [Zn]

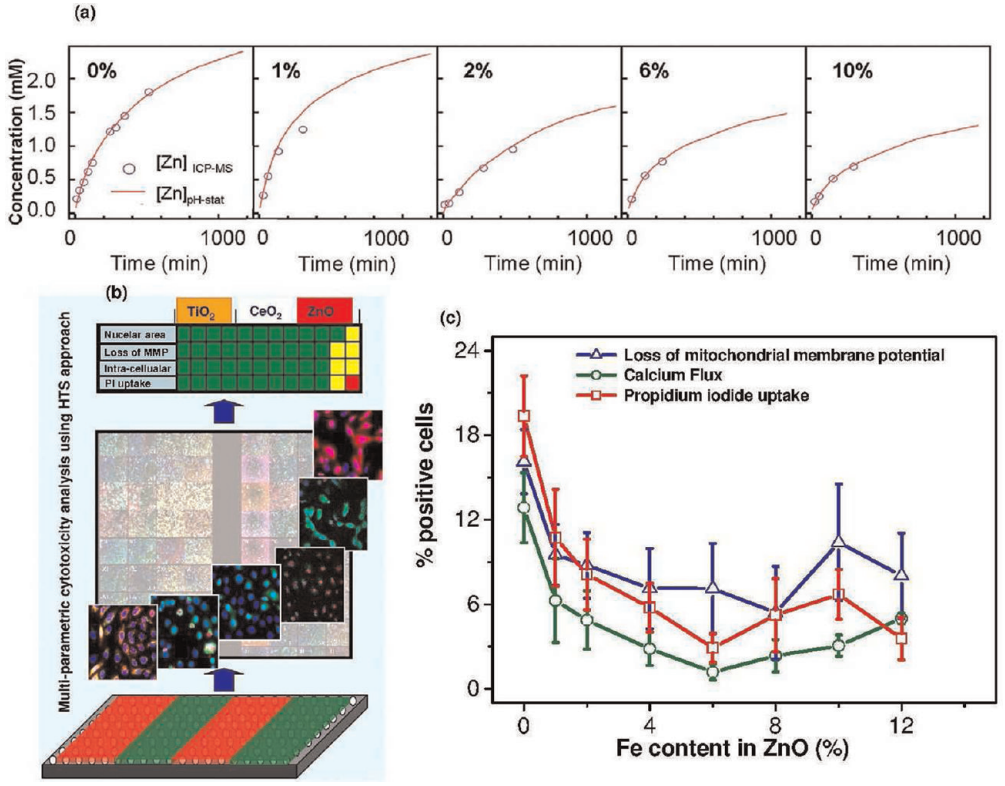

FIGURE 2. (a) Dissolution kinetics of pure or Fe doped ZnO NPs. (b) Toxicity evaluation for ZnO, CeO_2, or TiO_2 with fluorescent dyes. (c) Toxicity reduction with increase in Fe content in ZnO (safe-by-design strategy). (Reprinted in part with permission from ref 12. Copyright 2010 American Chemical Society.)

analysis using inductively coupled plasma mass spectrometry (ICP-MS). The results show that the concentration of Zn^{2+} released by the undoped NPs rapidly exceeds the saturation of Zn^{2+} for bulk ZnO (the bulk solubility product $K_{sp} = 11.2$ implies $[Zn]^{eq} = 1.58$ mM). The Zn^{2+} release is reduced through Fe incorporation into the crystal lattice of ZnO. The inner-shell Fe-*L* edge at 708 eV gives rise to an intense fine transition responsible for overlapping of the electron cloud from the neighboring atoms for interatomic bonding. The relatively strong σ-bonding of Fe in the host lattice of ZnO significantly reduces ZnO nanoparticle dissolution.

Electronic Properties and Dissolution of ZnO NPs Based Toxicity

The reduced dissolution of ZnO NPs is explained through the electronic properties of the engineered NPs. The results of a first-principles calculations show that Fe is substituted in Zn position.[20] The formation energy of Fe in ZnO suggests substitutional doping is strongly favorable for +2 oxidation state. The double Fe^{2+} substitution is more stable ($2Fe_{subs}$= −1.14 eV) compared with the single Fe^{2+} substitution ($1Fe_{subs} = -0.97$ eV).[20] The lattice geometry is changed by 0.03 Å in bond lengths and by 0.2° in bond angles after 10% Fe doping. Since d^6 configuration (Fe^{2+}) requires strong ligand field to cause spin paring in the tetracoordinated system[21] (high spin and low spin are assigned with the number of existing paired or unpaired electron in the e_g or t_{2g} orbitals), the low spin and completely occupied (Figure 1c,d) *d*-electrons are observed in Zn and doped Fe, respectively.[20] Consideration of the crystal field splitting of the Fe-3d states implies that Fe^{2+} is more strongly bound with O than Zn^{2+}.

The ZnO dissolution (51% to 26% from 0% to 10% Fe doping respectively, Supporting Information) was found to play a key role for the induction of the cellular cytotoxicity (Figure 2a).[18,22] The ZnO dissociation gives rise to increased [Zn] in the cell leading to mitochondrial damage followed by cell death. The cellular uptake as well as the material characteristics responsible for the oxidative stress determines the toxicological outcome (Figure 2b). The hierarchical oxidative stress model is associated with the level of inflammation experienced by the cell during NP exposure. Lower oxidative stress is associated with the induction of antioxidant enzymes. At higher levels of oxidative stress, the cell experiences inflammation and cytotoxicity. Inflammation is initiated through the activation of proinflammatory

signaling cascades such as mitogen-activated protein kinase (MAPK) and nuclear factor kB (NF-kB). The cell death could result from mitochondrial perturbation and the release of proapoptotic factors. The results show Zn^{2+} release is associated with ROS production and the oxidative stress pathways including intracellular calcium flux, mitochondrial depolarization, and plasma membrane leakage. After successful demonstration of the NPs dissolution induced intracellular toxicity, the engineering of ZnO NPs by iron doping led to significant reduction in toxicity proportional to the level of doping (Figure 2c).[12] Furthermore, these engineered NPs were also tested with higher organisms such as rodent and zebrafish models to conclusively establish reduced toxic effects in vivo.[19] The toxicity in the zebrafish was evaluated in terms of embryo hatching, mortality rates, and the generation of morphological defects.[19] Fe-doping interfered in the inhibitory effects of Zn^{2+} on a zebrafish hatching enzyme (due to the chelating property of Zn^{2+}). The toxicity assessment in the rodent lung included inflammatory cell infiltrates, lactate dehydrogenease (LDH), release and cytokine levels. The interference of inhibitory effects of Zn^{2+} by Fe doping was associated with decreased PMN cell counts, MCP-1 production, and increase in albumin levels in the mouse and rats.[19]

The results of the NPs toxicity in the in vivo sea urchin[23] showed that Fe-doped ZnO was less soluble than pure ZnO NPs. However, in contrast to the reduced toxicity observed in the in vitro cell culture system, no significant difference between toxicity with Fe-doped ZnO and the pure ZnO NPs was observed. The results show that the toxicity of the engineered NPs varies from organism-to-organism and from medium-to-medium. Despite reduced solubility and higher aggregation rates of Fe-doped ZnO NPs in seawater at environmentally relevant concentrations, the morphological abnormalities in developing sea urchin embryos was induced.[24] The toxicity is also mediated through Zn^{2+} dissolution like in the mammalian cell lines. The results highlight the importance of toxicity assessments both in vitro and in vivo, in numerous species and environmental media.

The exposure of ZnO NPs in different cell lines induces oxidative stress (through Zn^{2+} dissolution), leading to lipid peroxidation, membrane leakage, disruption of Ca^{2+} homeostasis, and ultimately cellular apopotosis.[12,18,19] In vivo studies in different organisms support oxidative stress due to ZnO NPs exposure.[25] Poynton et al. reported[26] that different gene expression profiles observed for ZnO NP suspensions and $ZnSO_4$ solutions point toward ZnO dissolution induced toxicity in *D. magna*. However, other studies found that antioxidant response genes were not induced after ZnO NP exposure. Huang et al. reported only few antioxidant genes responding to ZnO NP in human lung epithelial cells.[27] In another report, although ZnO NP exposure resulted in increased reactive oxygen species (ROS), zebrafish embryos failed to initiate an antioxidant response. They inferred that the cell does not recognize ZnO NPs as Zn^{2+} and therefore does not mobilize a response comparable to Zn^{2+} treatments.[25] However, once inside the cell, the NPs were capable of generating ROS and causing increased toxicity. In any case, the results suggest the need to conduct in-depth studies on the mechanism of the dissolution and the cellular outcome. To investigate this in more detail, degradation of the Fe−S containing proteins might be considered as a model example for the toxicity induction since Zn^{2+} is a metal ion which can easily chelate many bioligands in the cell containing Fe−S clusters.

The Zn^{2+} Interaction with Fe−S Redox Clusters

Extensive investigation on different mammalian cell lines showed that ZnO NPs dissolution played a major role in the toxicity generation. The reports on intracellular particle studies using in situ X-ray fluorescence (μXRF), X-ray absorption near edge structure (XANES), and synchrotron radiation X-ray fluorescence (SR-XRF) indicated that ZnO toxicity was caused by free or complexed Zn^{2+} within the cells, and not by reactions occurring on the surfaces of internalized solid phase NPs.[28] Hence, it is important to understand the effect of Zn^{2+} mobility in the cell in terms of interaction or chelation with different chemical species such as cellular proteins. A model for Zn^{2+} mobility and the possible cellular reactions with the Fe−S protein cluster are presented in Figure 3. Though Fe−S clusters can be chemically reconstituted, virtually all organisms contain a highly conserved, complex assembly and transfer system that facilitates the biogenesis of Fe−S cluster containing proteins.[29−31] The rhombic [2Fe-2S], cuboidal [3Fe-4S], and cubane [4Fe-4S] clusters interacting with Zn^{2+} (due to ZnO NPs dissolution and effective binding with the cell organelles, Supporting Information) leads to altered cellular responses in the cells.[32] Other common oxides such as silica and copper oxide exhibit similar behavior at elevated levels.[33,34]

In addition, when the ZnO NP is exposed to the cell, (1) the Zn^{2+} directly opens permeability transition (PT) pores, leading to depolarization, mitochondrial swelling, and cytochrome *c* release. Mitochondrial dysfunction (depletion of ATP) also leads to increase in ROS.[35] (2) The $[4Fe-4S]^{2+}$, one of the Fe−S clusters in the family of acotinase protein, is

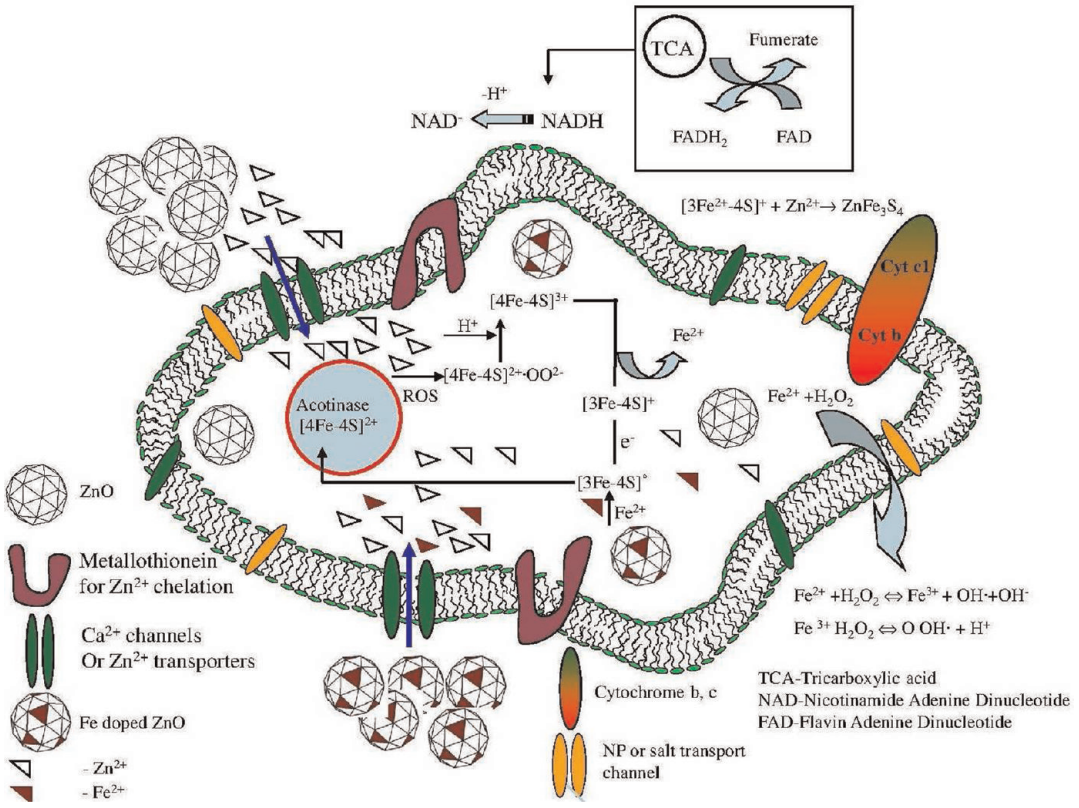

FIGURE 3. The Fe–S cluster degradation and respective charge transfer during the cellular Fe–S cluster metabolism through ZnO exposure and rectification of the protein with subsequent Fe addition through doped ZnO NPs. The channels in the cell membranes enhance the ions to migrate inside the cell for complex reactions as shown in the figure.

highly sensitive to oxidation and is damaged by ROS.[36] The oxidation of $[4Fe–4S]^{2+}$ by ROS produces an intermediate product $[4Fe–4S]^{2+}.OO^{2-}$ which reacts with available proton giving $[4Fe–4S]^{3+}$. The $[4Fe–4S]^{3+}$ cluster releases[37] Fe^{2+}, giving rise to hierarchical OS[11] eventually producing inactive $[3Fe–4S]^{0}$ after univalent reduction of $[3Fe–4S]^{3+}$.[38] (3) In vitro studies have also revealed that Zn^{2+} reacts not only with previously assembled iron–sulfur clusters but also with the unstable iron–sulfur clusters during biosynthesis.[39] The cellular properties with respect to decrease in the iron counts are due to the combination of Zn^{2+} with Fe–S cluster to give $ZnFe_3S_4$ (a product[40] from the reaction of Zn^{2+} and degraded cluster). (4) Regeneration of the active $[4Fe–4S]^{2+}$ in the cell is efficiently achieved through the reduction of the oxidized cluster and subsequent insertion of a ferrous ion from Fe-doped ZnO (iron pool) to rectify further cytotoxicity. Our results of ZnO and Fe doped ZnO NPs on the activity of Fe–S containing proteins showed that the citrate was isomerized into isocitrate, which was converted to α-ketoglutarate in a reaction catalyzed by isocitric dehydrogenase. These reactions were monitored through measuring the increase in absorbance at 340 nm associated with the formation of NADPH where the rate was proportional to protein activity. The rate of enzyme activity was also lowered significantly after addition of ZnO compared to the increased rate of enzyme activity after addition of Fe doped ZnO. Jang and Imlay reported the electron transfer from the iron–sulfur cluster because the reaction with H_2O_2 generates unstable $[4Fe–4S]^{3+}$ moieties in *Escherichia coli*. The cluster gained stability by releasing Fe^{2+} to form inactive $[3Fe–4S]^{+}$. Damaged clusters were reassembled chemically with dithiothreitol and Fe^{2+} treatment, where 60% activity was regenerated within 3 min.[41] The result shows a possible regeneration of the active protein moiety by the univalent reduction of the oxidized cluster and subsequent insertion of a ferrous ion from a Fe doped ZnO also in the mammalian cell lines to steer the cell into normal functioning as described in the present model (Figure 3). In summary, the mechanistic understanding of ZnO nanoparticle toxicity was addressed by flame aerosol engineered (Fe-doped) materials yielding less soluble particles that offer an improved safety margin. In-depth understanding of mechanisms of nanobiointeractions is required to develop such safe-by-design strategy through addressing details of the cellular functions and metabolisms.

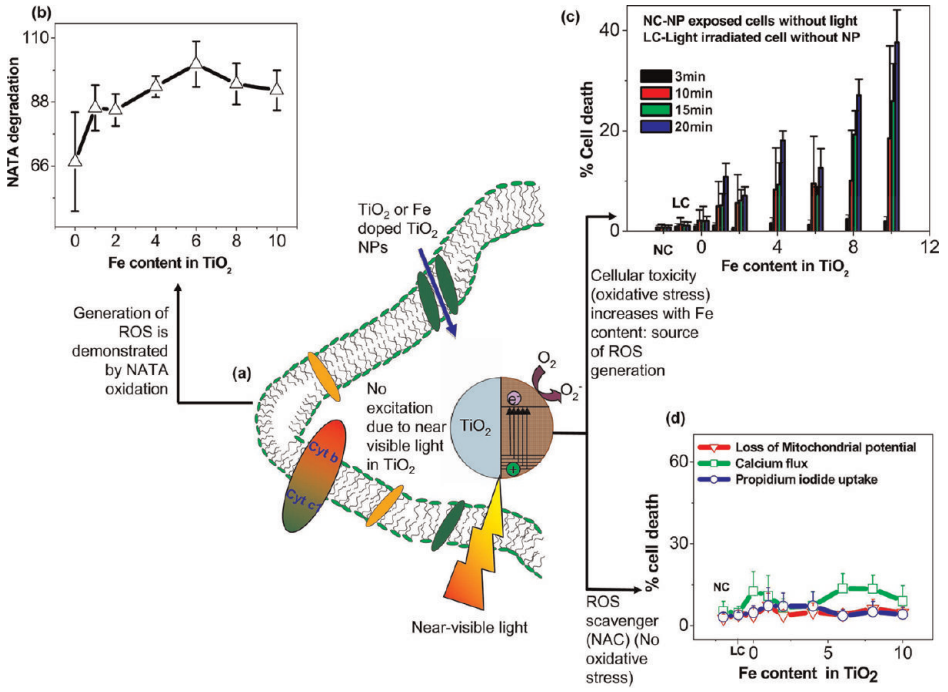

FIGURE 4. Near-visible light induced ROS and evidence of the oxidative stress. (a) Near-visible light irradiation of TiO_2 or Fe doped TiO_2 NPs in the cell. (b) ROS causing NATA degradation in the cell. (c) High throughput screening (HTS) used to determine cell death accompanied by various oxidative stress pathways. (d) Oxidative stress scavenger (NAC) for demonstrating the reduction of the phototoxicity. Adapted with permission from ref 45. Copyright 2011 American Chemical Society.

Apart from NPs dissolution induced oxidative stress, light induced phototoxicity is another oxidative stress paradigm.[42] UV can excite electrons into the conduction band of the NPs such as TiO_2 creating an electron−hole pair.[42] The generated charge interacts with H_2O and molecular oxygen to generate HO• radicals and superoxides.[43] However, the intrinsic toxic effects of light with high energy wavelengths responsible for the e^-/h^+ pair generation is a challenge in determining the potential phototoxicity of TiO_2. TiO_2 is reported as a strong candidate for the biological injury even in the absence of light because the conduction band is situated almost to the same level of the oxidative stress potential [$O_2 + e^- \rightarrow O_2^-$ ($E^\circ = -4.3$ eV), E° = standard electrode potential].[44]

Since FSP was versatile in engineering ZnO NPs by Fe doping, a TiO_2 based NP library (undoped or Fe doped) was synthesized using flame spray pyrolysis (FSP).[45,46] Results showed Fe loading was able to lower the band gap energy ($\Delta E_{TiO_2} = 3.2$ eV to $\Delta E_{\text{Fe-doped } TiO_2} = 2.8$ eV) through introduction of trap levels between the valence and conduction bands.[45] These trap levels allow for excitation of electrons when subjected to near-visible (350−450 nm) light illumination. The results of the NPs exposed cells with near visible light showed the increase in Fe loading increased the percentage of cell death (Figure 4).

The independent experiments performed for the verification of the ROS generation during light irradiation in the cell (Figure 4a) showed the following: (a) spontaneous degradation (Figure 4b) of *N*-acetyl-L-tryptophanamide (NATA), a biomolecule used for ROS capture during photochemical reactions in the cells, (b) multiparameter responses (superoxide generation, loss of mitochondrial membrane potential (MMP), and PI uptake) increased with Fe content (Figure 4c), and (c) cells pretreated with N-acetyl cysteine (NAC, a free radical quencher) failed to show any ROS in the cell. This is a clear indication of the light induced ROS responsible for the bioreaction and phototoxicity (oxidative stress) in the cell.

In summary, the radical generation from light activated NPs in the cell is responsible for the phototoxicity. The specific design using FSP appears to be instrumental for band gap tuning and the introduction of trap levels for electron capture during light exposure. With the proven ability of FSP to obtain fine particles and the phototoxicity evaluation method, the present concept of toxicity determination can be generalized for other photoactive materials.

Future Outlook for Designing Safer Nanoparticles and the State-of-the-Art of Double Flame FSP

In the past decade nanoscale materials have been prepared using a single flame reactor. Compared to the single flame setup, the stereoscopic two-flame reactor has further

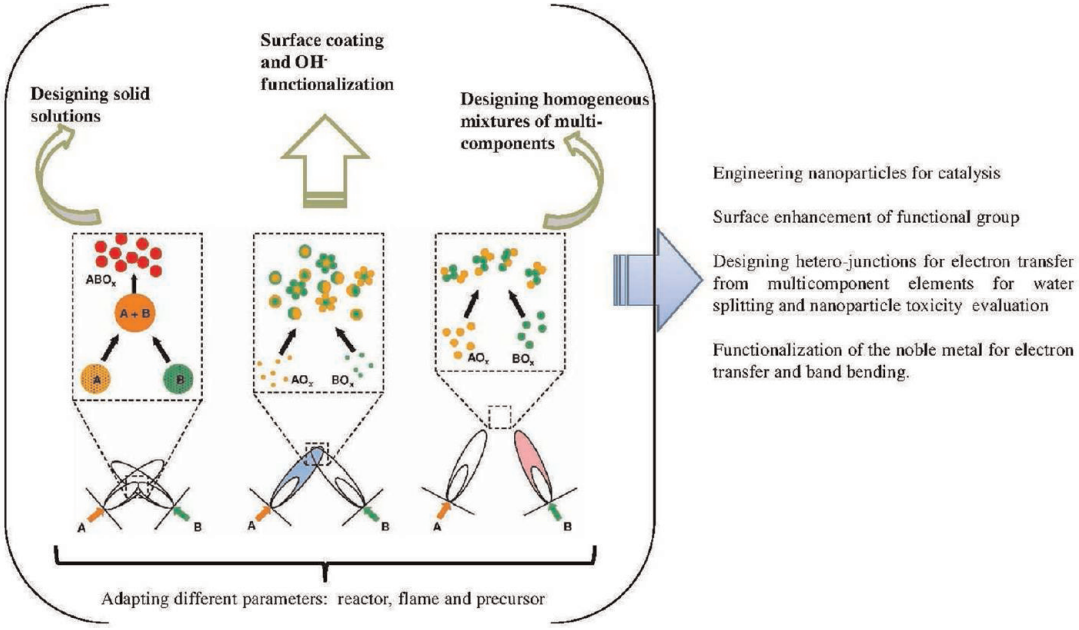

FIGURE 5. Versatile two reactor systems and the flame symmetry of flame spray pyrolysis for designing next generation nanoscale materials.

advantages such as flexibility for the control of important flame parameters affecting particle formation, and affording the control of particle mixing at the nanolevel in multicomponent systems. In the double flame approach, the particles are designed in two independent flames before the nanoparticles are collected (see Figure 5). The manipulation of the nozzle distance, the flame angles, and the defined distance at which two particle streams intersect give rise to innumerable possibilities for engineering nanoparticles for different applications. The double flame approach was first used by Strobel and co-workers to synthesize Pt loaded Ba/Al_2O_3 multicomponent catalyst for NO_x storage.[47−49] Minnermann et al. used two individual flames in tuning the alumina and cobalt oxide Fischer−Tropsch catalysts.[50] The individual components were individually controlled in each flame with respect to composition and size through adjusting the intersection distance of the flame. Such investigations on the influence of the intersection distances are rare in designing nanoparticles for different applications. The thermodynamically favorable inactive spinels such as $CoAl_2O_4$, $FeAl_2O_4$, Fe_2SiO_4, and Co_2SiO_4 that are not reduced at the catalysts operating temperatures are major phases produced during the material synthesis. These spinels were efficiently avoided by tuning the flame angles and the particle stream intersection distances.[50] Moreover, the double flame reactor also enables the homogeneous active metal dispersion with control over particle size and chemical aggregation. In another example, FSP was utilized for the preparation of Pd-silica/alumina system for tuning Brønsted acid sites on the surface of the nanoparticles. The density of the Brønsted acid sites could be tuned with the incorporation of the differing aluminum content in the vicinity of a silanol group.[51] These inherent acid sites could be tailored for varying pH of the cellular medium during toxicity testing. Recent developments based on molecular and/or nanostructure designs have led to advances toward light-induced charge separation and subsequent catalytic water oxidation and reduction reactions.[52] Developing nanoscale material, that focus on the development of visible-light active heteronanostructures is possible using double flame setup. If more than one type of nanoparticle is interacting in the environment, there can be protecting effects against ROS reduction or there might be metal ion adsorption or even incorporation into the second nanoparticle. However, there can also be more severe effects introduced by electron transfer between the NP and the intermediate reactions (antenna effect). This can be effectively studied using versatile double flame system for efficient in situ mixing of the nanoparticles at the nanolevel forming heterojunction for effective charge transfer.

Conclusion

The rapid multiparametric screening assessment shows that ZnO and TiO_2 are toxic due to particle dissolution and shedding of toxic Zn^{2+} and e^-/h^+ pair generation after irradiating with visible light, respectively. ZnO toxicity is reduced through Fe doping which leads to a stabilization

of crystal structure. In contrast, Fe doping increases the phototoxicity. Overall, our study demonstrates the utility of integrated cytotoxicity screening assays to assess nanomaterial hazard as well as to improve material safety through rational modification. The Fe which is doped in both the NPs (TiO_2 and ZnO) using the versatile FSP system changed the material property with respect to toxicity. From the results obtained for ZnO and TiO_2, it is clear that nanoscale materials need to be engineered to harvest intrinsic properties. The innovation in designing new particles lies in manipulating the reactor systems where the reaction parameters can be effectively controlled. Compared to the single flame setup, the two-flame reactor has innumerable advantages such as control over flame parameters, homogeneous multicomponent mixing, and control over nozzle distances (designing the intersection point of the two independent particle stream) and flame angle. To effectively design nanoparticles, a future outlook and the state of the art of the double flame FSP is described.

This material is based upon the work supported by the National Science Foundation and the Environmental Protection Agency under Cooperative Agreement Number DBI-0830117. Any opinions, findings, and conclusions or recommendations expressed in this material are those of the author(s) and do not necessarily reflect the views of the National Science Foundation or the Environmental Protection Agency. This work has not been subjected to EPA review and no official endorsement should be inferred. Key support was provided by the U.S. Public Health Service Grants U19 ES019528 (UCLA Center for NanoBiology and Predictive Toxicology), RO1 ES016746, and RC2 ES018766. We thank Prof. J. I. Zink, Dr. T. Xia, and Dr. S. George, CEIN, UCLA, for the useful discussion. We also thank Prof. A. Rosenauer and Dr. M. Schowalter, Department of Physics for Microscopic measurements. We are thankful to Dr. J. Birkenstock, Department of Geology, University of Bremen and Dr. H. J. Zhang, IWT, Foundation Institute of Material Science, University of Bremen for discussion.

Supporting Information. Experimental methods. This material is available free of charge via the Internet at http://pubs.acs.org.

BIOGRAPHICAL INFORMATION

Suman Pokhrel received his Ph.D. with JNU Fellowship in 2005 from the Madras University, India. He joined School of Chemistry and Materials Science, Heilongjiang University, China for his postdoctoral work in the year 2005–2006. He was awarded a Georg Forster Fellow of AvH Foundation in the Tübingen University, Germany in 2006. Presently he is working as a Research scientist in the Foundation Institute of Materials Science in the group of Prof. Lutz Mädler, University of Bremen. His research interests include synthesizing oxide nanostructured materials for various applications using soft chemistry routes and flame spray pyrolysis (FSP).

André E. Nel, Professor of Medicine and Chief, Division of NanoMedicine at UCLA, directs the University of California Center for the Environmental Impact of Nanomaterials and UCLA center for Nanobiology and Predictive Toxicology. He obtained his M.D. and doctorate degrees from Stellenbosch University in Cape Town, South Africa. His chief research interests are nano-EHS, nanobiology, and nanotherapeutics.

Lutz Mädler received his Ph.D. from Univ. Freiberg/Sa., Germany in 1999 and received his Habilitation in 2003 at Swiss Federal Institute of Technology (ETH Zurich). He was Senior Lecturer at the Department of Chemical Engineering, University of California, before he joined the Department of Production Engineering at the University of Bremen leading the Particle and Process Technology division in 2008. He is also Director at the Foundation Institute of Materials Science. His research focuses on integrated aerosol processes for nanomaterials and surface films for sensors, catalysts, and optical devices, and on nano-biointeractions.

FOOTNOTES

*To whom correspondence should be addressed. Mailing address: IWT, Foundation Institute of Material Science University of Bremen, 28359, Bremen, Germany. E-mail: lmaedler@iwt.uni-bremen.de. Phone: 00-49-(0)421-218-51200. Fax: 00-49-(0)421-218-51211.
The authors declare no competing financial interest.

REFERENCES

1 Joner, E. J.; Hartnik, T.; Amundsen, C. E. *Nanoparticles and the environment (TA-2304/2007)*; Bioforsk, Ås., 2007; pp 1–64.
2 Xia, Y. Nanomaterials at work in biomedical research. *Nat. Mater.* **2008**, *7* (10), 758–760.
3 Buzea, C.; Pacheco, I. I.; Robbie, K. Nanomaterials and nanoparticles: Sources and toxicity. *Biointerphases* **2007**, *2* (4), MR17–MR71.
4 Niederberger, M. Nonaqueous Sol-gel routes to metal oxide nanoparticles. *Acc. Chem. Res.* **2007**, *40* (9), 793–800.
5 Pokhrel, S.; Simion, C. E.; Teodorescu, V. S.; Barsan, N.; Weimar, U. Synthesis, mechanism, and gas-sensing application of surfactant tailored tungsten oxide nanostructures. *Adv. Funct. Mater.* **2009**, *19* (11), 1767–1774.
6 Teoh, W. Y.; Amal, R.; Mädler, L. Flame spray pyrolysis: an enabling technology for nanoparticles design and fabrication. *Nanoscale* **2010**, *2* (8), 1324–1347.
7 Pokhrel, S.; Birkenstock, J.; Schowalter, M.; Rosenauer, A.; Mädler, L. Growth of ultrafine single crystalline WO_3 nanoparticles using flame spray pyrolysis. *Cryst. Growth Des.* **2010**, *10* (2), 632–639.
8 Kemmler, J. A.; Pokhrel, S.; Birkenstock, J.; Schowalter, M.; Rosenauer, A.; Nicolae Bârsan, N.; Udo Weimar, U.; Mädler, L. Quenched, nanocrystalline $In_4Sn_3O_{12}$ high temperature phase for gas sensing applications. *Sens. Actuators B* **2012**, *161* (1), 740–747.
9 Nel, A. E.; Mädler, L.; Velegol, D.; Xia, T.; Hoek, E. M. V.; Somasundaran, P.; Klaessig, F.; Castranova, V.; Thompson, M. Understanding biophysicochemical interactions at the nano-bio interface. *Nat. Mater.* **2009**, *8* (7), 543–557.
10 Hussain, S. M.; Braydich-Stolle, L. K.; Schrand, A. M.; Murdock, R. C.; Yu, K. O.; Mattie, D. M.; Schlager, J. J.; Terrones, M. Toxicity evaluation for safe use of nanomaterials: recent achievements and technical challenges. *Adv. Mater.* **2009**, *21* (16), 1549–1559.
11 Nel, A.; Xia, T.; Mädler, L.; Li, N. Toxic potential of materials at the nanolevel. *Science* **2006**, *311* (5761), 622–627.
12 George, S.; Pokhrel, S.; Xia, T.; Gilbert, B.; Ji, Z. X.; Schowalter, M.; Rosenauer, A.; Damoiseaux, R.; Bradley, K. A.; Mädler, L.; Nel, A. E. Use of a rapid cytotoxicity screening approach to engineer a safer zinc oxide nanoparticle through iron doping. *ACS Nano* **2010**, *4* (1), 15–29.
13 Dürr, O.; Duval, F.; Nichols, A.; Lang, P.; Brodte, A.; Heyse, S.; Besson, D. Robust hit identification by quality assurance and multivariate data analysis of a high-content, cell-based assay. *J. Biomol. Screening* **2008**, *12* (8), 1042–1049.

14 Dahl, J. A.; Maddux, B. L. S.; Hutchison, J. E. Toward greener nanosynthesis. *Chem. Rev.* **2007**, *107* (6), 2228–2269.

15 Mädler, L.; Stark, W. J.; Pratsinis, S. E. Rapid synthesis of stable ZnO quantum dots. *J. Appl. Phys.* **2002**, *92* (11), 6537–6540.

16 Mueller, R.; Mädler, L.; Pratsinis, S. E. Nanoparticle synthesis at high production rates by flame spray pyrolysis. *Chem. Eng. Sci.* **2003**, *58* (10), 1969–1976.

17 Wegner, K.; Prastinis, S. E. Flame synthesis of nanoparticles. *Chem. Today* **2004**, *22* (6), 27–29.

18 Xia, T.; Kovochich, M.; Liong, M.; Mädler, L.; Gilbert, B.; Shi, H.; Yeh, J. I.; Zink, J. I.; Nel, A. E. Comparison of the mechanism of toxicity of zinc oxide and cerium oxide nanoparticles based on dissolution and oxidative stress properties. *ACS Nano* **2008**, *2* (10), 2121–2134.

19 Xia, T.; Zhao, Y.; Sager, T.; George, S.; Pokhrel, S.; Li, N.; Schoenfeld, D.; Meng, H.; Lin, S.; Wang, X.; Wang, M.; Ji, Z.; Zink, J. I.; Mädler, L.; Castranova, V.; Lin, S.; Nel, A. E. Decreased dissolution of ZnO by iron doping yields nanoparticles with reduced toxicity in the rodent lung and zebrafish embryos. *ACS Nano* **2011**, *5* (2), 1223–1235.

20 Xiao, J.; Kuc, A.; Pokhrel, S.; Schowalter, M.; Parlapalli, S.; Rosenauer, A.; Frauenheim, T.; Mädler, L.; Pettersson, L. G. M.; Heine, T. Evidence for Fe^{2+} in wurtzite coordination: iron doping stabilizes ZnO nanoparticles. *Small* **2011**, *7* (20), 2879–2886.

21 Cotton, F. A.; Wilkinson, G.; Murrillo, C. A.; Bochmann, M. *Advanced Inorganic Chemistry*, 6th ed.; John Wiley & Sons, Inc.: 1999; pp 776−814.

22 Damoiseaux, R.; George, S.; Li, M.; Pokhrel, S.; Ji, Z.; France, B.; Xia, T.; Suarez, E.; Rallo, R.; Mädler, L.; Cohen, Y.; Hoek, E. M. V.; Nel, A. No time to lose-high throughput screening to assess nanomaterial safety. *Nanoscale* **2011**, *3* (4), 1345–1360.

23 Fairbairn, E. A.; Keller, A. A.; Mädler, L.; Zhou, D.; Pokhrel, S.; Cherr, G. N. Metal oxide nanomaterials in seawater: Linking physicochemical characteristics with biological response in sea urchin development. *J. Hazard. Mater.* **2011**, *192* (3), 1565–1571.

24 Li, M.; Pokhrel, S.; Jin, X.; Mädler, L.; Damoiseaux, R.; Hoek, E. M. V. Stability, bioavailability, and bacterial Toxicity of ZnO and iron-doped ZnO nanoparticles in aquatic media. *Environ. Sci. Technol.* **2011**, *45* (2), 755–761.

25 Wong, S.; Leung, P.; Djurišić, A.; Leung, K. Toxicities of nano zinc oxide to five marine organisms: influences of aggregate size and ion solubility. *Anal. Bioanal. Chem.* **2010**, *396* (2), 609–618.

26 Poynton, H. C.; Lazorchak, J. M.; Impellitteri, C. A.; Smith, M. E.; Rogers, K.; Patra, M.; Hammer, K. A.; Allen, H. J.; Vulpe, C. D. Differential gene expression in daphnia magna suggests distinct modes of action and bioavailability for ZnO nanoparticles and Zn ions. *Environ. Sci. Technol.* **2011**, *45* (2), 762–768.

27 Huang, C.-C.; Aronstam, R. S.; Chen, D.-R.; Huang, Y.-W. Oxidative stress, calcium homeostasis and altered gene expression in human lung epithelial cells exposed to ZnO nanoparticles. *Toxicol. In Vitro* **2010**, *24* (1), 45–55.

28 Gilbert, B.; Fakra, S. C.; Xia, T.; Pokhrel, S.; Mädler, L.; Nel, A. E. The Fate of ZnO nanoparticles administered to human bronchial epithelial cells. *ACS Nano* **2012**, *6* (6), 4921–4930.

29 Mansy, S. S.; Cowan, J. A. Iron-sulfur cluster biosynthesis:toward an understanding of cellular machinery and molecular mechanism. *Acc. Chem. Res.* **2004**, *37* (9), 719–725.

30 Holm, R. H. Synthetic approaches to the active sites of iron-sulfur proteins. *Acc. Chem. Res.* **1977**, *10* (12), 427–434.

31 Seefeldt, L. C.; Dean, D. R. Role of nucleotides in nitrogenase catalysis. *Acc. Chem. Res.* **1997**, *30* (6), 260–266.

32 Volbeda, A.; Charon, M.-H.; Piras, C.; Hatchikian, E. C.; Frey, M.; Fontecilla-Camps, J. C. Crystal structure of the nickel-iron hydrogenase from desulfovibrio gigas. *Nature* **1995**, *373* (6515), 580–587.

33 Brunner, T. J.; Wick, P.; Manser, P.; Spohn, P.; Grass, R. N.; Limbach, L. K.; Bruinink, A.; Stark, W. J. In vitro cytotoxicity of oxide nanoparticles: comparison to asbestos, silica, and the effect of particle solubility. *Environ. Sci. Technol.* **2006**, *40* (14), 4374–4381.

34 Studer, A. M.; Limbach, L. K.; Van Duc, L.; Krumeich, F.; Athanassiou, E. K.; Gerber, L. C.; Moch, H.; Stark, W. J. Nanoparticle cytotoxicity depends on intracellular solubility: comparison of stabilized copper metal and degradable copper oxide nanoparticles. *Toxicol. Lett.* **2010**, *197* (3), 169–174.

35 Gazaryan, I. G.; Krasinskaya, I. P.; Kristal, B. S.; Brown, A. M. Zinc irreversibly damages major enzymes of energy production and antioxidant defense prior to mitochondrial permeability transition. *J. Biol. Chem.* **2007**, *282* (33), 24373–24380.

36 Flint, D. H.; Tuminello, J. F.; Emptage, M. H. The inactivation of iron-sulphur cluster containing hydro-lyases by superoxide. *J. Biol. Chem.* **1993**, *268* (30), 22369–76.

37 Leal, S. N. S.; Gomes, C. U. M. Linear three-iron centres are unlikely cluster degradation intermediates during unfolding of iron-sulfur proteins. *Biol. Chem.* **2005**, *386* (12), 1295–1300.

38 Gardner, P. R.; Raineri, I. s.; Epstein, L. B.; White, C. W. Superoxide radical and iron modulate aconitase activity in mammalian cells. *J. Biol. Chem.* **1995**, *270* (22), 13399–13405.

39 Iwasaki, T. Iron-sulfur world in aerobic and hyperthermoacidophilic archaea *Sulfolobus*. *Archaea* **2010**, *2010*, 842639.

40 Srivastava, K. K. P.; Surerus, K. K.; Conover, R. C.; Johnson, M. K.; Park, J. B.; Adams, M. W. W.; Munck, E. Mössbauer study of zinc-iron-sulfur $ZnFe_3S_4$ and nickel-iron-sulfur $NiFe_3S_4$ clusters in pyrococcus furiosus ferredoxin. *Inorg. Chem.* **1993**, *32* (6), 927–936.

41 Jang, S.; Imlay, J. A. Micromolar intracellular hydrogen peroxide disrupts metabolism by damaging iron-sulfur enzymes. *J. Biol. Chem.* **2007**, *282* (2), 929–937.

42 Hoffmann, M. R.; Martin, S. T.; Choi, W.; Bahnemann, D. W. Environmental applications of semiconductor photocatalysis. *Chem. Rev.* **1995**, *95* (1), 69–96.

43 Sinha, R. P.; Hader, D. P. UV-induced DNA damage and repair: a review. *Photochem. Photobiol. Sci.* **2002**, *1* (4), 225–236.

44 Burello, E.; Worth, P. A. A theoretical framework for predicting the oxidative stress potential of oxide nanoparticles. *Nanotoxicology* **2010**, *5* (2), 228–235.

45 George, S.; Pokhrel, S.; Ji, Z.; Henderson, B. L.; Xia, T.; Li, L.; Zink, J. I.; Nel, A. E.; Mädler, L. Role of Fe doping in tuning the band gap of TiO_2 for the photo-oxidation induced cytotoxicity paradigm. *J. Am. Chem. Soc.* **2011**, *133* (29), 11270–11278.

46 Teoh, W. Y.; Amal, R.; Mädler, L.; Pratsinis, S. E. Flame sprayed visible light-active Fe-TiO_2 for photomineralisation of oxalic acid. *Catal. Today* **2007**, *120* (2), 203–213.

47 Strobel, R.; Krumeich, F.; Pratsinis, S. E.; Baiker, A. Flame-derived Pt/Ba/$Ce_xZr_{1-x}O_2$: Influence of support on thermal deterioration and behavior as NOx storage-reduction catalysts. *J. Catal.* **2006**, *243* (2), 229–238.

48 Strobel, R.; Mädler, L.; Piacentini, M.; Maciejewski, M.; Baiker, A.; Pratsinis, S. E. Two-nozzle flame synthesis of Pt/Ba/Al_2O_3 for NOx storage. *Chem. Mater.* **2006**, *18* (10), 2532–2537.

49 Strobel, R.; Pratsinis, S. E. Flame aerosol synthesis of smart nanostructured materials. *J. Mater. Chem.* **2007**, *17* (45), 4743–4756.

50 Minnermann, M.; Großmann, H.; Pokhrel, S.; Thiel, K.; Hagelin-Weaverd, H.; M. Bäumer, M.; Mädler, L. Double flame spray pyrolysis as a novel technique to synthesize alumina-supported cobalt Fischer−Tropsch catalysts. *Catal. Today* **2012**, *Manuscript submitted.*

51 Huang, J.; van Vegten, N.; Jiang, Y.; Hunger, M.; Baiker, A. Increasing the Brønsted acidity of flame-derived silica/alumina up to zeolitic strength. *Angew. Chem., Int. Ed.* **2010**, *49* (42), 7776–7781.

52 Tachibana, Y.; Vayssieres, L.; Durrant, J. R. Artificial photosynthesis for solar water-splitting. *Nat. Photonics* **2012**, *6*, 511–518.